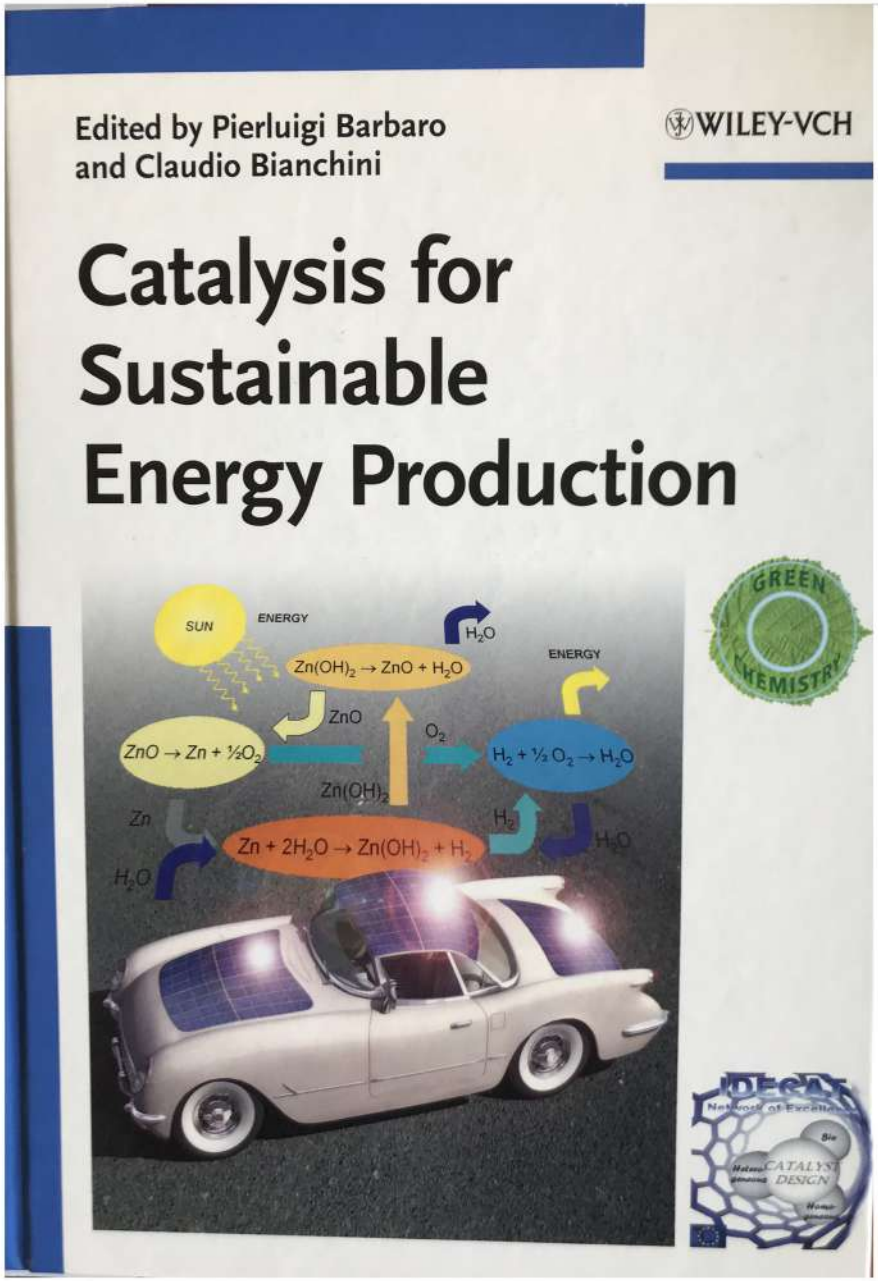

4
Towards Full Electric Mobility: Energy and Power Systems*

Pietro Perlo, Marco Ottella, Nicola Corino, Francesco Pitzalis, Mauro Brignone, Daniele Zanello, Gianfranco Innocenti, Luca Belforte, and Alessandro Ziggiotti

4.1
Introduction

The purpose of this chapter is to quantify the technological advances and the timing of their introduction towards cleaner and more efficient vehicles based on electric propulsion.

4.2
The Current Grand Challenges

The transport sector is responsible for almost 60% of oil consumption in OECD (Organization for Economic Cooperation and Development) countries, it is a major source of pollution and greenhouse gas emissions and it is the chief sector driving future growth in world oil demand [1]. Mobility is currently based almost 100% on hydrocarbons, whether fossil fuels or combustible from renewables (liquids and gases). Most continents have an increasing dependence on primary energy; for instance, Europe is forecasting 70% by 2030 [2]. Of comparable relevance for Europe is the growing dependence on raw materials such as aluminum and steel, generating large uncertainties in forecasting, and made even worse by the global economic instability.

The concern for primary energy is dominant while demanding increased safety and reduced noxious and greenhouse emissions, with the following expectations: fewer than 35 000 annual fatalities in Europe by 2010 while aiming at fewer than 100 fatalities per million vehicles by 2015, with radical reductions of both NO_x and CO_2 emissions and aiming at zero local emissions [3].

Amongst novel opportunities (or constraints), the automotive industry will be faced with the following [4]:

*A List of Symbols can be found at the end of this chapter.

Catalysis for Sustainable Energy Production. Edited by P. Barbaro and C. Bianchini

ISBN: 978-3-527-32095-0

- People and goods will increase their need of mobility by ~35% per decade for at least 3–4 decades.
- The number of mega-cities is increasing and most of the traffic will be urban.
- Urban centers are more and more congested and closed to traffic.
- Mobility is related to invariants such as the following: people move for 1 h per day – the average speed, since it was measured for the first time in 1923, remains stable in the range 35–40 km h^{-1} – people tend to relate mobility to mental freedom and according to the US Bureau of Transportation as many as 90% of kilometers covered are run in vehicles with a single occupant.
- Just in Europe an extra one million cars come on the road every 50 days and globally the number of vehicles is projected to rise from 900 million in 2007 to 2200 million by 2050.
- The emerging markets require low-cost and environmentally compatible vehicles.

Possible answers to the above challenges extend through a reduction in system complexity (an ordinary car can have more than 50 processors, actuators and sensors), novel concepts for personal mobility and advanced systems integration towards a more electric and to full electric mobility. The following sections address these issues.

4.3 Power–Energy Needed in Vehicles

4.3.1 Basic Formulation

In its simplest form, neglecting the losses due to road camber and curvature, the power required at the drive wheels (P_{total}) may be expressed as follows [5]:

$$P_{total} = P_{kin} - P_{grade} + P_{air\text{-}drag} + P_{tire\text{-}friction} \tag{4.1}$$

where P_{kin} is the power required for acceleration, P_{grade} the power required for the gradient, $P_{air\text{-}drag}$ the power consumed by the aerodynamic drag and $P_{tire\text{-}friction}$ the rolling resistance power consumed by the tires. The first two terms describe the rates of change of potential (PE) and kinetic (KE) energy during climbing and acceleration, respectively, and can be calculated as follows:

$$P_{kin} = \frac{d(KE)}{dt} = \frac{d\left(\frac{1}{2}Mv^2\right)}{dt} = Mav \tag{4.2}$$

$$P_{grade} = \frac{d(PE)}{dt} = Mgv \sin q \tag{4.3}$$

where M is the mass (kg) of the car, v its velocity (m s^{-1}), a its acceleration (m s^{-2}) and $\tan q$ the gradient. The potential and kinetic energy acquired by the car as a result of

climbing and acceleration can, in principle, be recovered by regenerative methods whereby the mechanical energy is converted and stored as electric energy.

The power required to overcome tire friction and aerodynamic drag is irreversibly lost, mainly as heat and noise, cannot be recovered and can be estimated from the following empirical relations:

$$P_{air\text{-}drag} = \frac{1}{2}\rho C_x S v^3 \tag{4.4}$$

$$P_{tire\text{-}friction} = \mu M g v \tag{4.5}$$

where μ and C_x are dimensionless tire friction and aerodynamic drag coefficients, respectively, ρ the air density (kg m^{-3}), v the velocity of the car (m s^{-1}), g (= 9.8 m s^{-2}) the acceleration due to gravity and S the frontal cross-sectional area (m^2) of the car.

If η_{drive} is the overall electric powertrain efficiency, the instantaneous total electric power delivered by the accumulators is given by

$$P_{accumulators} = \frac{P_{total}}{\eta_{drive}} + P_{accessories} \tag{4.6}$$

and the total energy to stored in the accumulators by

$$E_{total} = \partial P_{accumulators} dt + E_{idle} \tag{4.7}$$

where E_{idle} is the energy consumed by the powertrain at idle. E_{total} depends on the drive cycle chosen as reference and in practice, for a specific cycle up to 30% of the consume, could depend on the driver's attitude.

In the remainder of this chapter we will refer to the New European Driving Cycle (NDEC), described in Figure 4.1, consisting of four urban cycles at a maximum speed of 50 km h^{-1} and one suburban cycle at a maximum speed of 120 km h^{-1}.

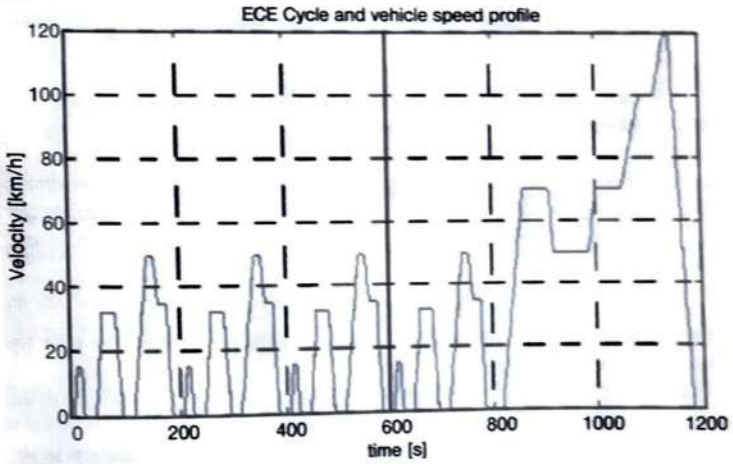

Figure 4.1 NDEC cycle.

4.3.2
Well to Wheel Evaluations

Within the automotive industries, the methodology mostly referred to for a first comparison between the performances of different powertrain technologies is the so-called Well to Wheel analysis. This approach compares vehicle and powertrains starting from a reference not specifically optimized for the new technologies and, consequently, the results are not based on the best possible input parameters for the selected technology (for instance, a user in the case of an electric vehicle could be electronically assisted for efficient driving much more than it could be by a conventional internal combustion engine (ICE) powertrain associated with a full mechanical transmission). In spite of that, Well to Wheel analyses are meaningful and necessary, at least at first glance, as they consider the different chemical energy carriers on the basis of their true energy content or the higher heating value (HHV) of all fuels considered [6].

We refer here to the analysis reported in the EUCAR website extended to an ideal electric powertrain [7]. The results for a 100 km drive in NDEC cycles reported in Figure 4.2a show that, independently of where the electricity is produced, the electric powertrain is associated with radical primary energy savings, similarly, and consequently, to radical control of noxious and greenhouse gas emissions (Figure 4.2b).

It is worth noting that even the most optimistic case, hydrogen fuel cells that consider hydrogen produced in the vicinity of the distributor, require a higher need for primary energy than natural gas internal combustion engines adopting heavy gas tanks. Even neglecting the energy and the time necessary to generate the infrastructures, the current challenge on primary energy and the rapid advances in electric energy storage would suggest whether it could still be under discussion to focus research and development toward powertrain solutions adopting more electrics towards the final goal of full electric vehicles based on batteries and supercapacitors.

4.3.3
Specific Calculations for Ideal Electric Powertrains

With the purpose of understanding the performance of an ideal electric powertrain vehicle, we now apply the formulations described in Section 4.3.1 to calculate the energy necessary to be stored in batteries while varying the vehicle mass and aerodynamic factor SC_x.

The hypotheses are as follows:

- Drive and braking are made by electric motors having efficiency maps with an average of 90%.
- Braking energy is preferably recovered in supercapacitors with an efficiency of 90%.
- The first phase of the acceleration in the NDEC cycle is driven by supercapacitors.
- Electric cabling and power electronics have an overall efficiency of 95%.

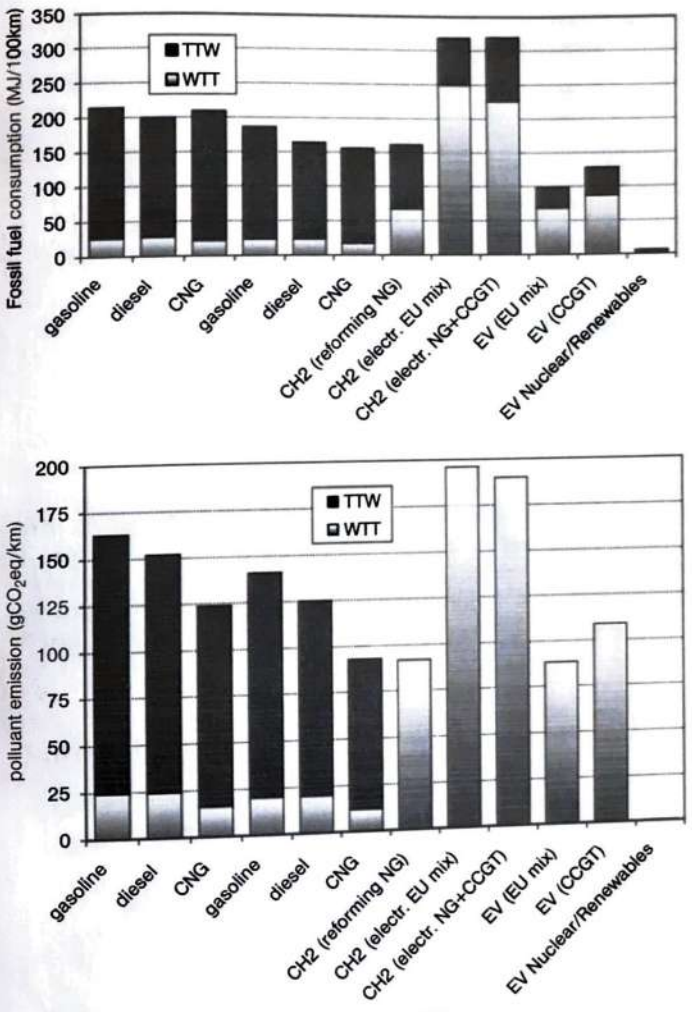

Figure 4.2 Well to Wheel analysis of (a) primary energy consumption for conventional and electric vehicles and (b) CO_2 emissions for conventional and electric vehicles.

Figure 4.3 shows the results for covering a total of 10 NDEC cycles (100 km). While a small-sized car of total weight 800 kg and $SC_x = 0.55\,m^2$ require ~14 kW h, a medium–large-sized car of 1500 kg and $SC_x = m^2$ would require an energy of 27 kW h, almost twice as much.

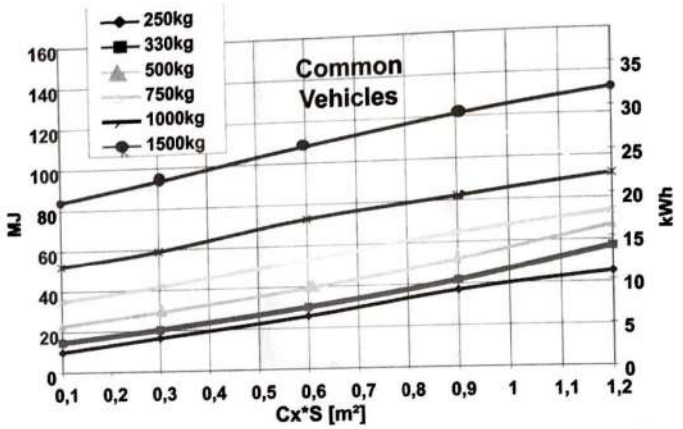

Figure 4.3 Influence of weight and shape on the energy needed to run an electric efficient car.

When designing an electric vehicle, the first question is the dimensions of the electric motor(s) in relation to the required performance. With that in mind, in Figure 4.4 the iso-power lines refer to the total nominal power required at the motors to reach a speed of 120 km h^{-1}. The typical peak power of an electric motor could be as much as 2–3 times the nominal power and the graph should then be used for

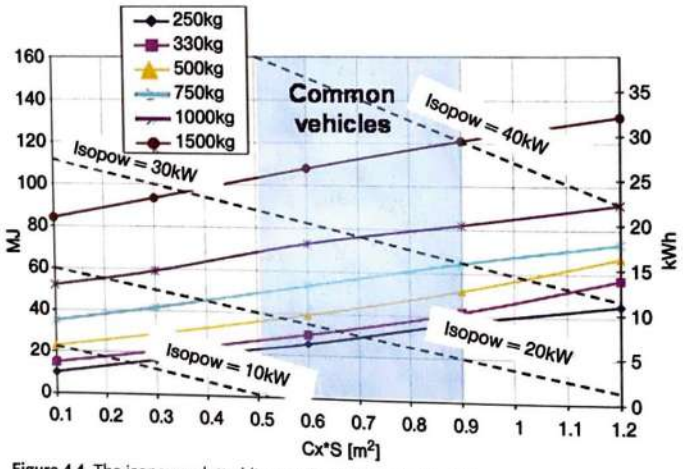

Figure 4.4 The isopower dotted lines indicate that a lightweight electric efficient car can be run with a total nominal power in the region of 10 kW; in contrast, a 1500 kg car would require as much as three to four times that power.

reference only, but in any case it is clear that a narrow superlight vehicle can be driven robustly with a total nominal power of less than 10 kW whereas a medium–large vehicle may require as much as 30–40 kW.

The control of both mass and shape is crucial for radical energy savings and also to reduce the overall complexity in motor design, cooling, electronic control and overall electric cabling.

4.3.4
A Roadmap of Feasibility with Batteries and Supercapacitors

To understand the evolution of the electric accumulators, let us consider a vehicle with a mass of 500 kg and aerodynamic factor $SC_x = 0.6\ m^2$. Figure 4.5 shows that for a range of 400 km in NDEC cycles the necessary energy to be delivered by the batteries is of about 34 kW h. In the hypothesis of full depth of charge and discharge by state-of-the-art methods available in the 1997, the overall weight of the batteries needed was 675 kg (a trailer behind the car), whereas in 2007 it was 168 kg, more technically feasible, and conservative projections anticipate only 84 kg before 2020.

Referring to the Battery Association of Japan [8], in the period 1990–2005 the energy density of commercial batteries increased 5.2-fold (Figure 4.6). The typical commercial automotive Li-P batteries rank at 200 W h kg^{-1} and continuing with only half the current rate of advance the electric powertrain from 2017 on is very likely to be lighter and cheaper than the best solutions based on ICEs, fuel, tank, mechanical transmissions and gears.

- Total vehicle mass: 500kg
- Autonomy: 400km = 40cycles

C_x*S	Necessary energy	
[m²]	[MJ]	[kWh]
0.6	122	33.89

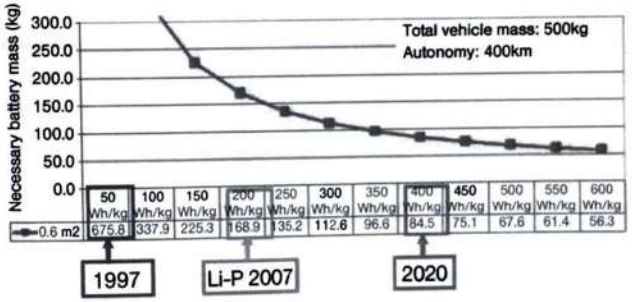

Figure 4.5 On the basis of the current predictions on battery development, the necessary battery mass for a 500 kg vehicle for a range of 400 km in NDEC cycles (120 km h^{-1}) is projected to be lower than the overall weight of a conventional powertrain based on an internal combustion engine.

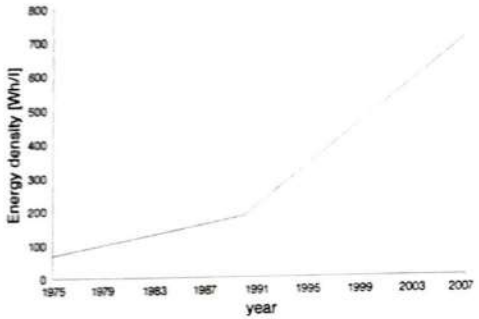

Figure 4.6 In the last 15 years, the energy density of batteries has increased 5.8-fold.

4.3.5 The Need for Range Extenders

Although the effect of the mass can be partly reduced by adopting efficient recovery systems, when driving at high speeds the range would be rather limited even for a lightweight vehicle. Figures 4.7 and 4.8 show the calculations of the power required at constant speeds of 50 and 120 km h^{-1}. At low speed the power of the motors is such that with less than 100 kg of batteries there would be an autonomy of several hours for all usual cars. At speeds above120 km h^{-1}, typical on main highways, for an acceptable autonomy, reduced weight and cost of batteries, a fuel-based range extender is necessary unless the car could be particularly lightweight and with a small aerodynamic factor.

A typical scheme of a serial powertrain configuration including a range extender is shown in Figure 4.9. The range extender, that is, a fuel-based electric generator, can be connected directly to the motors and/or used to charge the accumulators continuously. Figure 4.10 compares the possible options of range extenders in terms of their specific power and efficiency.

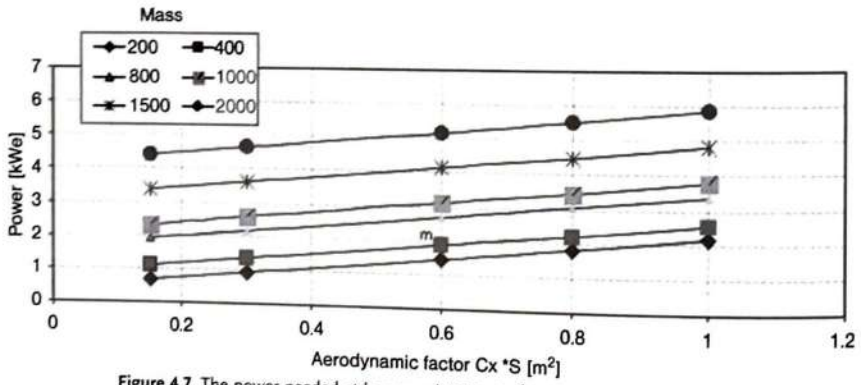

Figure 4.7 The power needed at low speed (50 km h^{-1})is low independently of the mass, thus allowing a long range of the vehicle.

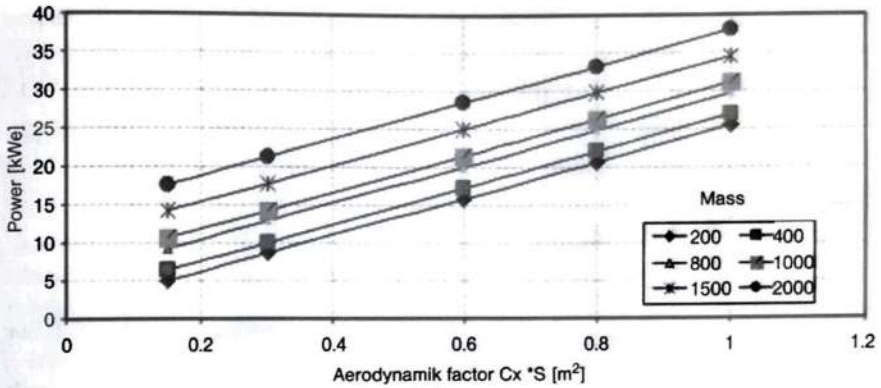

Figure 4.8 The power needed at high speed (120 km h^{-1})is relatively high independently of the mass, limiting the range of the vehicle.

Amongst the various options, the fuel cell is the most promising in that it is intrinsically scalable, maintaining high efficiency at both low and high powers, and further it is modular in that from a basic module the total power can be increased to any level by connecting several modules in series. On the negative side it has a relatively low power density and therefore it is usually coupled with a supercapacitor

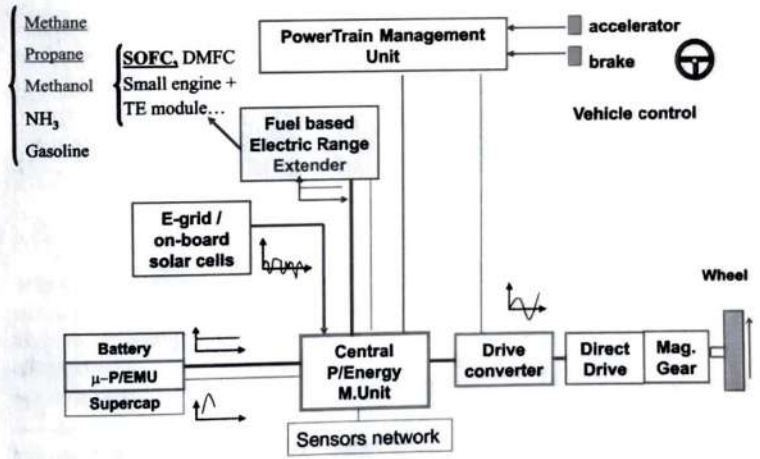

Figure 4.9 General scheme of a serial hybrid electric vehicle where the range extender is used either to drive the motors or to charge the accumulators.

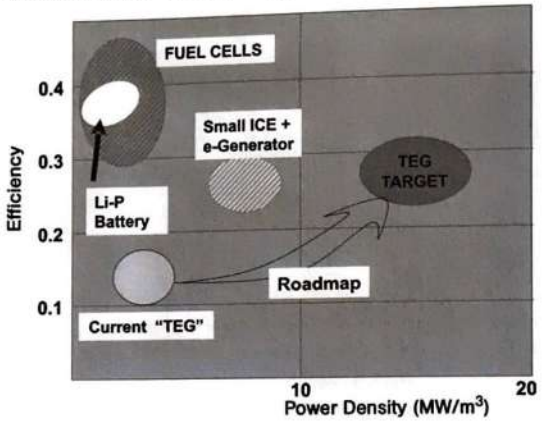

Figure 4.10 Direct thermoelectric generators will compete in efficiency with internal combustion engines when thermoelectric materials with figures of merit ZT of the order of 2 are available at temperatures above 900 K.

set. The ICE is difficult to operate at high efficiency when designed at relatively low powers and, in addition, it needs to be coupled to an electric generator, but on the positive side it is associated with a fairly well-developed technology. Stirling engines could be a further option in that, when used as range extenders, their intrinsic limitations of slow startup and low power density can be compensated with supercapacitors. Continuous operation is an interesting factor because they can have similar efficiency to small ICEs while being simpler to manufacture.

The emerging technology of thermoelectric generators (TEGs), when designed with the purpose of directly generating electricity, is appealing in that, by using high thermoelectric materials with a 'figure of merit' above $ZT = 2$, it is scalable with efficiencies comparable to those of small ICEs. The power densities can be potentially high and the manufacturing prospects are rather simple. On the negative side, direct TEGs are still in their first phase of development. In the following section we describe specific advances in this technology.

4.3.5.1 Direct Thermoelectric Generators

In the last decade, much effort has been expended on developing novel thermoelectric (TE) materials of increased intrinsic conversion efficiency [9]; at same time, the design of the system architecture plays an important role in optimizing the thermal exchange and in maximizing the conversion performance [10]. For that reason, in this section we report an example of a detailed thermal management analysis with the heat re-flowed in the system.

The efficiency in TE power generation depends on the intrinsic characteristics of the material and on the temperature ratio between the hot and the cold sides [11]:

$$\eta_{TE} = \eta_{Carnot}\eta_{ZT} \tag{4.8}$$

where

$$\eta_{ZT} = \frac{\sqrt{1+ZT}-1}{\sqrt{1+ZT}+(T_c/T_h)} \tag{4.9}$$

and

$$\eta_{Carnot} = 1-\frac{T_c}{T_h} \tag{4.10}$$

where ZT is the 'figure of merit' of the TE material and, for commercial bismuth telluride modules operating at low temperature (273–373 K), it reaches a maximum value of 0.8 [12]. Higher performance materials working at higher temperatures, such as LAST-18 [13], can reach a value of $ZT \approx 2$ at about 750 K.

Here we will concentrate on system design and a typical value of $ZT = 1$ will be chosen for all working temperatures. The electric power generation as a fraction of the thermal heat flux is given by the generic relationship for thermal cycles [14]:

$$W = Q_h\eta_{TE} = Q_h\eta_{Carnot}\eta_{ZT} \tag{4.11}$$

where Q_h is the incoming heat flux from the high-temperature source set at 800 K to allow comparison between different system layouts. This is a typical temperature of combusted waste gases for which it is possible to build a system without special materials; of course, for a higher temperature the system would have a higher efficiency. We distinguish amongst systems with an isothermal hot side, with an isothermal cold side and with a temperature gradient on both sides. For a comparison of the different architectures, we refer to a detailed reported analysis [15].

For the sake of simplicity, without avoiding the rigor of the analysis, we describe only the combustion-driven architecture based on a counter-current exchanger layout (Figure 4.11).

The basic hypothesis is that the temperature profiles of the two flows are parallel. This means that the heat exchanged at the hot side equals that exchanged at the cold side. This is an approximation since extracting electric power from the heat flux implies a difference between the two heat fluxes. However, the hypothesis, with only a minor influence on the final result, makes the equations compact and easy to manage.

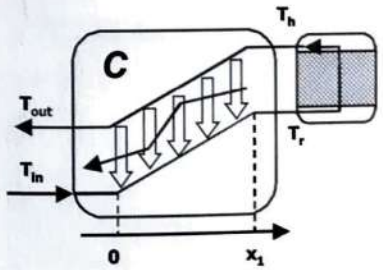

Figure 4.11 Counter-current exchanger layout for a TEG.

The temperature gap (ΔT) between the two flows is chosen as the controlling parameter: it determines both the enthalpy feed and the Carnot efficiency of the thermoelectric element. The value of ΔT is related to the heat exchanger efficiency η_{exc} or ε-NTU (normal thermal unit), the ratio of the heat exchanged to the total exchangeable heat. This relationship comes from the definition of ε-NTU for the exchanger efficiency and, in this specific case, it has the following form [16]:

$$\varepsilon\text{-NTU} = 1 - \frac{\Delta T}{T_h - T_{in}} \tag{4.12}$$

By solving the energy balance of the system, we obtain the total efficiency, given by

$$\eta_{tot} = \frac{W}{H_{in}} = \eta_{ZT} \ln\left(\frac{T_h}{T_{in} + \Delta T}\right) \tag{4.13}$$

The electric power over the mass flow rate of the working fluid is given by

$$W^1 = \Delta T \eta_{tot} = \Delta T \eta_{ZT} \ln\left(\frac{T_h}{T_{in} + \Delta T}\right) \tag{4.14}$$

These two functions are plotted in Figure 4.12; it can be seen that the total efficiency increases with the exchanger performance whereas the specific power reaches a maximum at about 0.53 of ε-NTU. The interesting result is that the efficiency of the counter-current exchanger exceeds the value of the intrinsic TE material efficiency η_{TE} (Equation 4.8, horizontal dotted line in Figure 4.12) in the high ε-NTU efficiency

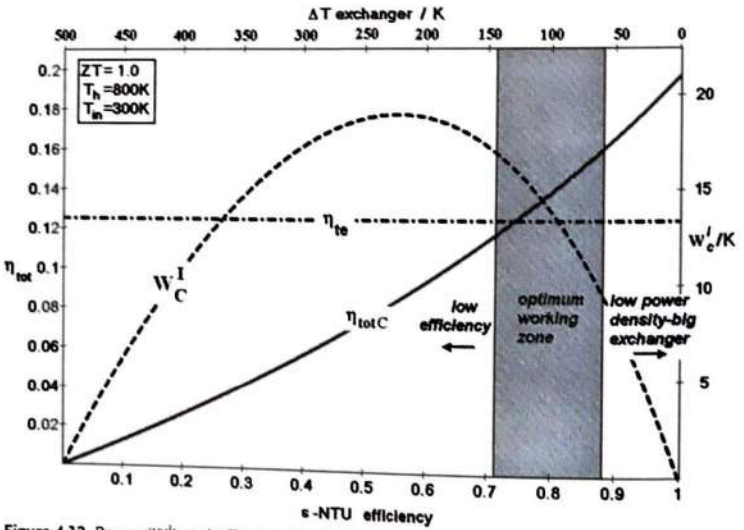

Figure 4.12 Power (W^1) and efficiency (η_{tot}) characteristics of a counter-current exchanger TEG system. For comparison, the intrinsic TE efficiency (η_{TE}) without heat recirculation is reported.

region. We can select an optimum working zone close to 80% of the heat exchange efficiency. Lower values lead to a low total efficiency whereas higher values imply low specific fluid power, high exchange area and more material and weight.

4.4
A Great New Opportunity for True Zero Emissions

A number of companies are currently involved in thin-film photovoltaics [17], and low-cost multilayer thin-film amorphous silicon and CdTe (cadmium telluride) systems have already been installed in large numbers with efficiencies of the order of 10% and of about 80% output after 25 years of operation. Large-scale plants have been announced for the so-called CIS (cadmium indium selenide) and CGIS (copper gallium indium diselenide), technologies with production efficiencies in the range 12–13% and laboratory measurements up to 19.9% [18].

Thin-film photovoltaics are projected at a cost below $\$100\,m^{-2}$ [18] and their integration in automotive bodies is a relatively easy process. An indication of this new possibility for true zero emission is shown in the following example: $3.5\,m^2$ of thin film having 12% efficiency, when in the open air in the north, center and south of Italy under the average daily irradiance over the year, would produce 1.52, 1.97 and 2.27 kW h per day, respectively. The last value is sufficient for a 600 kg efficient electric vehicle to run up to 20 km per day [19], which is just the range covered every day by more than 80% of people. Thin-film photovoltaics maintain a good response under diffused light [18] and, in the perspective of the forthcoming mass-produced transparent photovoltaic thin films, the daily harvested energy could be doubled. Figures 4.13 and 4.14 show the rendering of a car covered with thin-film PV that, when not in use and connected to the grid, becomes a source of extra income.

Figure 4.13 Car with integrated thin-film PV cells.

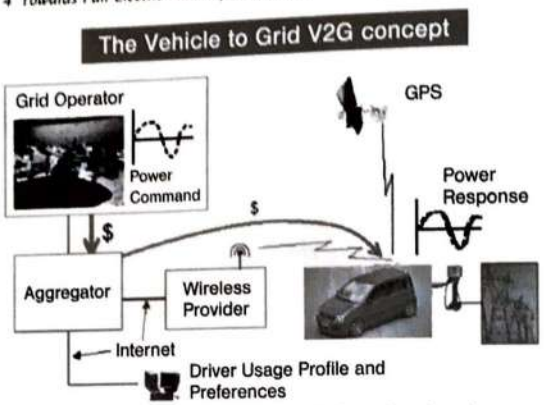

Figure 4.14 Vehicle to grid concept: the vehicle can be plugged into the grid to either buy or sell electricity.

4.5
Advanced Systems Integration

In systems with a power profile of both charge and discharge, power electronics is necessary to protect the batteries. The current state-of-the-art high energy density batteries do not like to be fully recharged or discharged quickly and then when used in the regenerative energy mode their efficiency and lifetime are reduced. In contrast, supercapacitors are robust and efficient devices that can provide round-trip efficiencies above 90% [20, 21].

For fast recharging of a battery, high currents of several tens of amperes are required, and necessarily robust designs and expensive materials such as titanium have to be used to sustain the stresses induced by the current flowing at temperatures that can exceed 120 °C [22]. The energy density is constrained at around 50% lower values than when optimized for maximum energy density. The final result for fast recharging is higher cost and greater weight.

While waiting for the next generation of superbatteries having both maximum power and energy density [20, 21], the integration of the optimum power and energy systems results in the most efficient, robust and cheapest solution for both hybrid and fully electric powertrains [22].

Partitioning of both supercapacitors and batteries into a number of cells has several advantages: high surface-to-volume ratio facilitating heat dissipation, higher degree of power and energy control while reducing the effects of malfunctions, and higher flexibility to locate the elements in the vehicles.

Similarly, referring to Figure 4.9, the electric motor, power electronic converter and DC–DC converter must be designed in a strongly coupled concept in order to achieve the characteristics required for the powertrain, summarized here in five attributes: high torque, high efficiency, lightweight, wide speed range and low cost. High efficiencies and high torque densities require the use of rare earth permanent magnets,

which are known to be very expensive; machines must be designed to minimize their weight. In addition, power electronics converters must be designed to exploit the highest efficiency figures of the machines. The forthcoming developments in power electronic modules (e.g. Silicon Carbide technology) and in the integration of several power and control modules into compact units will result in a noticeable increase in the overall efficiency of the electric powertrain in the range of 90% and above.

4.6
Conclusion and Perspectives

For the first time in the history of mobility, the technological advances in the overall system blocks within an electric powertrain have reached a level where full electric mobility can be possible. The overall system integration, that is, overall system optimization, plays a crucial role in that power and energy storage systems should preferably be coupled with advanced local management, drive electronics should be coupled with drive motors embedding torque control, while a central unit manages power and energy flows within the electric drive train.

The vehicle can be plugged in to the national grid for either buying or selling electricity and, in countries having high solar radiation such as southern Europe, a low-cost in-body photovoltaic thin film can provide free, clean energy for driving up to 40–50 km per day. In summary, the near- and mid-term perspectives can be grouped as follows:

Concerning the environment and health:

1. Lower CO_2 emissions independently from where the electricity is produced.
2. Lower NO_x and fine particle emissions (zero local emissions).
3. Reduced problems on recycling materials.

Concerning the shortage of resources and eliminate the need of new costly infrastructures:

4. Lower dependence on primary energy (less energy to produce a car and less to run it).
5. Lower weight: reduced use of raw materials such as aluminum and steel.
6. Available public infrastructures with low maintenance and simple private infrastructures.

Concerning economic mobility and fun-to-drive without restrictions:

7. Lower cost of vehicles at equal performance.
8. Better fun-to-drive (control of the torque).
9. Lower cost per kilometer (5–10 times less than an ICE at least until a new tax is applied).

Concerning new industrial opportunities:

10. New vehicles, electric generators, power electronic, batteries, supercaps, e-motors.
11. Radical reduction in the overall supply chain: raw materials–production–commercialization.

List of Symbols

C_p	specific heat of convective medium
$\dot{m}C_p$	specific heat rate of the convective medium
η_{tot}	system total efficiency
η_{exc}	heat exchanger efficiency ε-NTU
η_{TE}	thermoelectric element efficiency
η_{Carnot}	Carnot contribution to the efficiency
η_{ZT}	contribution of thermoelectric material to the efficiency
H_{in}	inlet enthalpy
T_h	hot side temperature
T_{in}	convective medium inlet temperature
T_{out}	outgoing convective medium temperature
W	electric power generated
W^l	specific power of the fluid
ΔT	temperature gap between flows in heat exchanger

Combustor

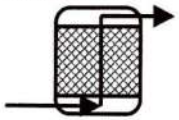

In this component the combustion of the air–fuel mixture takes place; also in this case the vertical line is proportional to the enthalpy feeding

Thermoelectric series

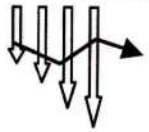

This symbol represents a heat flux (white arrows) from which an electric power (black arrow) is extracted by TE elements

Acknowledgments

Nicola Corino, Francesco Pitzalis and Daniel Zanello wish to acknowledge the Fondazione Cassa di Risparmio di Torino (FCRT) for providing fellowship support to complete their PhDs.

References

1 Energy Balances of OECD Countries, 2004–2005, 2007 edition, http://www.iea.org/Textbase/publications/free_new_Desc.asp?PUBS_ID=1931.
2 European Commission, Energy for the Future: Renewable Energy Sources, http://ec.europa.eu/energy/library/599fi_fr.pdf.
3 http://www.euresearch.ch/fileadmin/documents/PdfDocuments/Presentations/Pr_sentation_Transport January07.pdf.
4 http://www.ertrac.org/pdf/publications/ertrac_RF_brochure_june2006.pdf.
5 Shukla, A.K. (2001) *Resonance – Journal of Science Education*, **6** (11), 49–62;

Genta, G. Meccanica dell'Autoveicolo 2000, Levrotto e Bella edition.
6 Bossel, U. Well-to-Wheel Studies, Heating Values and Energy Conservation, www.efcf.com/reports/E10.pdf. Bossel, U. Phenomena, Fact and Physics of a Sustainable Energy Future, www.efcf.com.
7 http://www.eucar.be/start.html/publications/well to wheel study.
8 Battery Association of Japan, http://www.baj.or.jp/e/index.html.
9 Bell, L.E.PhD BSST, LLC5462 Irwindale Avenue, Irwindale CA 91706lbell@amerigon.com, 626.815.7430. Alternate Thermoelectric Thermodynamic Cycles with Improved Power Generation Efficiencies.
10 Rowe, D.M. (2006) *Thermoelectrics Handbook*, Taylor & Francis, Boca Raton, FL.
11 Goldsmid and Ioffe, A.F. (1957) *Semiconductor Thermoelements and Thermoelectric Cooling*, Infosearch, London.
12 Goldsmid, H.J., Sheard, A.R. and Wright, D.A. (1958) *British Journal of Applied Physics*, **9**, 365.
13 Hsu, K.F., Loo, S., Guo, F., Chen, W., Dyck, J.S., Uher, C., Hogan, T., Polychroniadis, E.K. and Kanatzidis, M.G. (2004) *Science*, **303**, 818.
14 Snyder, G.J. (2005) Thermoelectric power generation: efficiency and compatibility, in *Thermoelectrics Handbook: Macro to Nano* (ed. D.M. Rowe), CRC Press, Taylor & Francis, Boca Raton, FL, Chapter. 9.
15 Ziggiotti, A. (2007) Hydrogen thermoelectric microcombustors, PhD thesis.
16 Cengel, Y.A. (1996) *Introduction to Thermodynamics and Heat Transfer*, McGraw-Hill, New York.
17 http://www.nrel.gov/pv/thin_film/.
18 http://www1.eere.energy.gov/solar/thin_films.html.
19 Perlo, P. (2008) Smart systems integration for the forthcoming electric mobility, Proceedings of the 2008 Annual Forum of the IEEE-ISSCC Society, Power Systems from the GigaWATT to the MicroWatt – Generation, Distribution, Storage and Efficient Use of Energy, 8 February 2008, San Francisco.
20 Burke, A.F. (2007) Batteries and ultracapacitors for electric, hybrid and fuel cell vehicles, *Proceedings of the IEEE*, **95** (4), 806–820.
21 Ehsani, M., Gao, Y. and Miller, J.M. (2007) Hybrid electric vehicles: architecture and motor drives, *Proceedings of the IEEE*, **95** (4), 719–729.
22 Burke, A.F. (2007) Supercapacitors in hybrid vehicle powertrains, in Proceedings of TransAlpine Workshop on Hybrid, Electric and fuel Cell Systems, October 2007, Pollein, Italy.